remote sensing

MDPI

Article

Seasonal Variation in the NDVI–Species Richness Relationship in a Prairie Grassland Experiment (Cedar Creek)

Ran Wang [1,*], John A. Gamon [1,2,3,*], Rebecca A. Montgomery [4,†], Philip A. Townsend [5,†], Arthur I. Zygielbaum [3,†], Keren Bitan [4,†], David Tilman [4,†] and Jeannine Cavender-Bares [4,†]

1 Department of Earth and Atmospheric Sciences, University of Alberta, Edmonton, AB T6G 2E3, Canada
2 Department of Biological Sciences, University of Alberta, Edmonton, AB T6G 2E9, Canada
3 School of Natural Resources, University of Nebraska, Lincoln, NE 68583, USA; aiz@unl.edu
4 Department of Ecology, Evolution and Behavior, University of Minnesota, Saint Paul, MN 55108, USA; rebeccam@umn.edu (R.A.M.); knb47@cornell.edu (K.B.); tilman@umn.edu (D.T.); cavender@umn.edu (J.C.-B.)
5 Department of Forest and Wildlife Ecology, University of Wisconsin, Madison, WI 53706, USA; ptownsend@wisc.edu
* Correspondences: rw6@ualberta.ca (R.W.); jgamon@gmail.com (J.A.G.); Tel.: +1-780-807-3156 (R.W.); Fax: +1-780-492-2030 (R.W.)
† These authors contributed equally to this work.

Academic Editors: Susan L. Ustin, Parth Sarathi Roy and Prasad S. Thenkabail
Received: 2 December 2015; Accepted: 1 February 2016; Published: 5 February 2016

Abstract: Species richness generally promotes ecosystem productivity, although the shape of the relationship varies and remains the subject of debate. One reason for this uncertainty lies in the multitude of methodological approaches to sampling biodiversity and productivity, some of which can be subjective. Remote sensing offers new, objective ways of assessing productivity and biodiversity. In this study, we tested the species richness–productivity relationship using a common remote sensing index, the Normalized Difference Vegetation Index (NDVI), as a measure of productivity in experimental prairie grassland plots (Cedar Creek). Our study spanned a growing season (May to October, 2014) to evaluate dynamic changes in the NDVI–species richness relationship through time and in relation to environmental variables and phenology. We show that NDVI, which is strongly associated with vegetation percent cover and biomass, is related to biodiversity for this prairie site, but it is also strongly influenced by other factors, including canopy growth stage, short-term water stress and shifting flowering patterns. Remarkably, the NDVI-biodiversity correlation peaked at mid-season, a period of warm, dry conditions and anthesis, when NDVI reached a local minimum. These findings confirm a positive, but dynamic, productivity–diversity relationship and highlight the benefit of optical remote sensing as an objective and non-invasive tool for assessing diversity–productivity relationships.

Keywords: remote sensing; species richness; productivity; grassland; NDVI

1. Introduction

The species richness–productivity relationship has long been of interest in ecology. Much of the recent Biodiversity-Ecosystem Function (BEF) research has developed from a series of landmark experiments at Cedar Creek that consistently demonstrated that biodiversity enhances productivity in experimental grassland systems [1–3]. Two hypotheses have been proposed to explain the positive relationship between biodiversity and productivity: (1) selection effects; and (2) complementarity [4,5]. The selection effects hypothesis (also called "selection probability effects") states that adding species

increases the probability of having a productive species, especially when creating a community with high richness within a small size pool of candidate species [6]. The complementarity hypothesis suggests that the presence of multiple species in a high richness community can increase production via more efficient resource capture.

In reviews of the BEF literature, a variety of biodiversity–productivity relationships have been reported [7,8]. Both unimodal and positive relationships are commonly reported between productivity and richness, and this relationship can be affected by community composition, resource levels (e.g., fertilizer or irrigation levels) and nature of disturbance [8–10]. In some cases, highly productive sites are known to be resource rich and species poor. These high productivity and low diversity sites are typically highly managed via irrigation or fertilizer application [8] and often lead to declines in the species richness relationships at high productivity. Indeed, variation in the relationship between biodiversity and ecosystem function is known to depend on resource availability [11] and environmental drivers, particularly drought stress, has been shown to constrain biomass in prairie systems [12,13].

One goal of BEF research is to understand the underlying ecological mechanisms behind the biodiversity–productivity relationship. However, the assessment of the relationship itself and changes in the relationship through time pose additional challenges. Determining the nature of these relationships is of increasing importance in natural systems, given that unmanipulated grasslands show a range of productivity–diversity relationships, depending on site conditions and composition [7]. Prairie productivity is often estimated through biomass harvests that are time-consuming due to the effort in harvesting, sorting and weighing live vegetation in the sampling region [14–16]. There are also limits to the number of samples that can be taken in a single season without altering the experiment. Moreover, the traditional methods of estimating biomass - and their repeatability—can be subjective due to the dependence on the knowledge and skill of those conducting sampling [15]. This estimation is further affected by sample size and method [17]. Due to these constraints, only a small area can typically be harvested to obtain the biomass and richness. As a consequence, it has been difficult to observe changes in biomass in response to external drivers through time and the seasonal dynamics of the diversity–productivity relationship.

Remote sensing provides a useful tool to estimate vegetation productivity over large areas and has been used to estimate prairie production. A large number of studies have led to well-established methods that estimate the percent cover, biomass, and productivity of grasslands using remote sensing [14,15,18,19]. These studies have shown that the Normalized Difference Vegetation Index (NDVI) [20] is highly correlated with green biomass, green leaf area index, and radiation absorption (APAR) by green canopy material in grasslands [16,19]. Remote sensing also provides an objective method that can assess productivity rapidly, repeatedly and following consistent methods, without damaging or altering the target vegetation.

The Cedar Creek Ecosystem Science Reserve (CCESR; Minnesota, USA) has a long, rich history of biodiversity studies. The ongoing BioDIV experiment has been maintained for more than 20 years to investigate the effects of species and functional biodiversity on community and ecosystem function, and has included assessment of productivity, stability and nutrient dynamics [2,21]. Previous studies at this site have reported a significant, positive relationship between diversity (either species richness or functional diversity) and biomass (e.g., [2]).

In this study, we revisited the species richness–productivity relationship for these experimental prairie grassland plots covering a range of biodiversity levels (nominal species richness ranging from 1 to 16 plant species per plot) using NDVI, a common remote sensing metric of ecosystem productivity and green vegetation biomass. Our study spanned a summer growing season (May to October, 2014), allowing us to evaluate dynamic changes in the NDVI–species richness relationship through time and in relation to environmental variables, including temperature, precipitation and soil moisture. We tested the hypotheses that (1) remote estimates of productivity would be positively associated with species richness, as reported by previous studies based on traditional field sampling methods [2,3];

and (2) the relationship would change dynamically throughout the growing season in response to the progression of plants through shifting phenological stages and according to environmental fluctuations (e.g., as a consequence of summer drought).

2. Methods

2.1. Field Site and Experimental Design

This study was conducted at the Cedar Creek Ecosystem Science Reserve, Minnesota, US (45.4086° N, 93.2008° W). The BioDIV experiment has maintained 168 prairie plots (9 m × 9 m) with nominal plant species richness ranging from 1 to 16 since 1994 [22]. The species planted in each plot were originally randomly selected from a pool of 18 species typical of Midwestern prairie, including C_3 and C_4 grasses, legumes and forbs. Of the original 168 plots, 35 plots with species richness ranging from 1 to 16 were selected for our study. These 35 plots included 11 monoculture plots and six replicates of every other richness level (2, 4, 8, and 16) but with differing species combinations. Weeding was done 3 to 4 times each year for all the plots to maintain the species richness. A more complete accounting of the methods and history of the BioDIV experiment can be found in the published literature on this site (e.g., [1,23]).

2.2. Reflectance Sampling

In the 35 study plots, canopy spectral reflectance was measured every two weeks over most of the 2014 growing season (late May to late August) and once a month during senescence (September to October) with a hand-held, dual channel spectrometer (Unispec DC, PP Systems, Amesbury, MA, USA) (Figure 1a). With this instrument, both upwelling radiance and downwelling irradiance were collected simultaneously, and these measurements were cross-calibrated using a white reference calibration panel (Spectralon, Labsphere, North Sutton, NH, USA), allowing us to correct for the atmospheric variation [24]. The detectors measured irradiance and radiance from 350 to 1130 nm with a nominal bandwidth (band-to-band spacing) of approximately 3 nm, and actual bandwidth (FWHM) of 10 nm. The upward-looking channel included a fibre optic and a cosine head to record the solar irradiance. The downward-looking channel included a fibre optic and a field-of-view restrictor that limited the field of view (FOV) to a nominal value of 20 degrees, although empirical tests indicated the actual FOV was closer to 15 degrees (not shown). In this application, the spatial resolution on the ground (IFOV) was approximately 0.5 m^2. The reflectance at each wavelength was calculated as:

$$\rho_\lambda = \frac{\left(L_{target,\lambda}/E_{target,\lambda}\right)}{\left(L_{panel,\lambda}/E_{panel,\lambda}\right)} \quad (1)$$

where $L_{target,\lambda}$ indicates the radiance measured at each wavelength (λ , in nm) by a downward-pointed detector sampling the surface ("target"), and $E_{target,\lambda}$ indicates the irradiance measured simultaneously by an upward-looking detector sampling the downwelling radiation. $L_{panel,\lambda}$ indicates the radiance measured by a downward-pointed detector sampling the calibration panel, and $E_{panel,\lambda}$ indicates the irradiance measured simultaneously by an upward-pointed detector sampling the downwelling radiation.

A linear interpolation was applied to the reflectance spectra to obtain reflectance values at 680 and 800 nm and calculate NDVI:

$$NDVI = \frac{\rho_{800} - \rho_{680}}{\rho_{800} + \rho_{680}} \quad (2)$$

where ρ_{680} and ρ_{800} indicate the reflectance at 680 and 800 nm respectively. To determine seasonal NDVI patterns, 17 reflectance measurements were taken along the northern-most row on each sampling date (Figure 1a) in each of the 35 plots, providing a consistent subsample of each plot over the growing

season. To estimate the NDVI values on 1 August (the day that vegetation percent cover was measured) a linear interpolation was applied to NDVl measurements made on 18 July and 4 August.

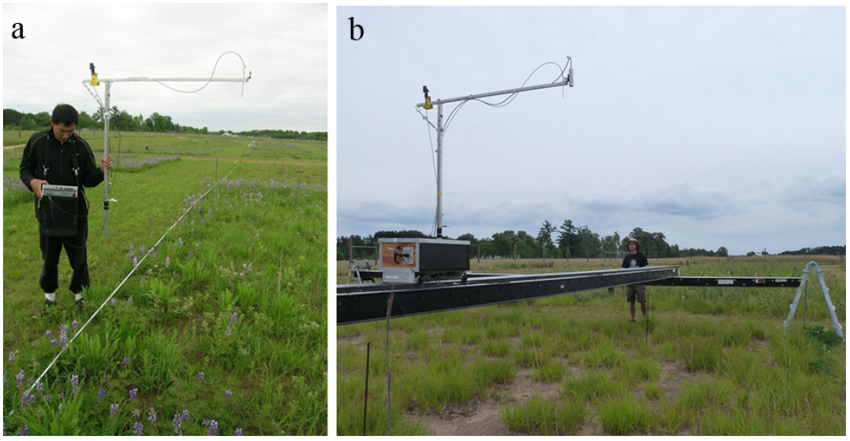

Figure 1. Sampling spectral reflectance using (**a**) the handheld method, applied biweekly to obtain reflectance phenology over the season; and (**b**) the tram cart on track [24] used to sample entire plots once near midsummer peak biomass. For the first method, only the northern-most row of each plot was sampled for reflectance phenology over the growing season. The second method is further illustrated in Figure 2.

2.3. Whole-Plot Reflectance Sampling

Once at peak season (23 July to 3 August), we sampled canopy reflectance of 33 entire plots using a tram system [24] (Figure 1b). The tram consisted of a mobile cart on a movable track supported by scaffolding (Figure 1b), allowing a systematic measurement of each 1-m^2 portion of each plot (Figure 2a). This resulted in a total of 81 measurements (9 × 9 m) for each plot with approximately 1 m^2 spatial resolution, creating a synthetic image (Figure 2b) that provided a full sample of each of the 33 plots, comparable to what could be obtained with airborne imaging spectrometry. The speed of the tram cart was 0.167 m/s. It took approx. 10 min (including time to move the scaffolding) to cover a plot (9 × 9 m). During the (whole-plot) sampling period, data were collected from 10 am to 4 pm every day until all 33 plots were completely sampled. We skipped midday (12:30 pm to 1 pm) to avoid possible self-shadow effects of the fiber when measuring the white reference. While some data reported were collected under clear skies, clouds were unavoidable, and their influence on NDVI calculations were largely reduced through the cross-calibration procedure described above. A quantum sensor (LI-190SB, LI-COR, Lincoln, NE, USA) was used to track the sky condition when running the tram cart. To avoid possible edge effects, 49 (7 × 7 m) of the 81 measurements in the center were used to calculate the average reflectance of each plot (Figure 2c). NDVI from each reflectance spectrum was calculated using Equation (2) and the average NDVI was determined for each plot.

2.4. Biomass and Vegetation Percent Cover

Above-ground living plant biomass of the selected 35 plots was measured on 4 August 2014. Plots were sampled by clipping, drying and weighing four parallel and evenly spaced 0.1 m × 6 m strips per plot. The biomass of each strip was sorted to species, but presented here as total plot biomass. Ground vegetation percent cover measurements were taken on 19 June and 1 August in 2014. Percent cover was determined by visual inspection within nine 0.5 m × 0.5 m quadrats, placed every meter, starting 50 cm from the north facing edge of the plot for a total of nine subsamples per plot. Percent cover was estimated for each individual species as the nearest 10 percent that each species occupied of the total quadrat area, and then summed. Vegetation coverage did not necessarily sum to 100% if bare ground was exposed, or if species overlapped. To avoid affecting seasonal NDVI patterns, biomass

measurements in each plot were sampled in a separate area from the reflectance sampling locations, both of which were assumed to be representative of the whole plot. For mid-season NDVI assessment of *entire* plots, the biomass sampling was conducted a few days after the optical sampling to avoid affecting the NDVI.

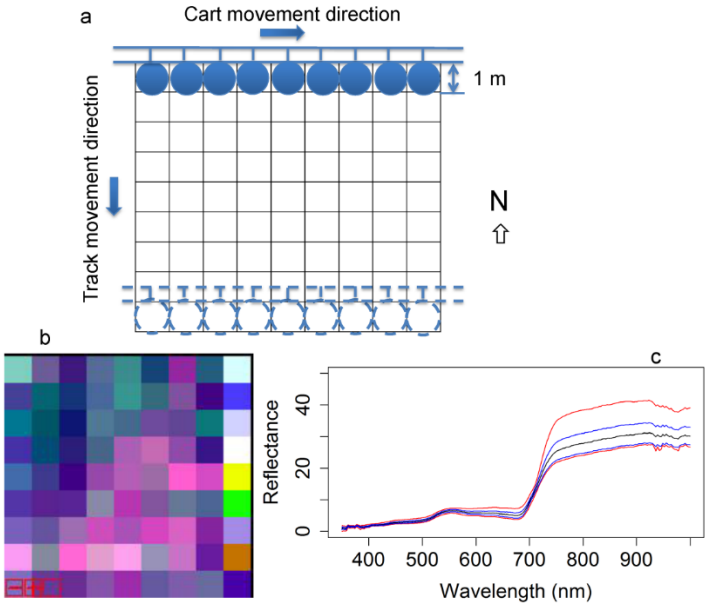

Figure 2. Design of whole-plot reflectance sampling (**a**) and example of synthetic image (plot 168, richness = 16) (**b**); and resulting reflectance spectra (**c**). Colored lines indicate mean (black), standard deviation (blue) and min/max (red) reflectance values. Reflectance spectra were used to calculate NDVI through time for comparison with nominal species richness (1–16).

2.5. Height

We monitored height of focal species at each NDVI census as an independent measure of canopy growth. We measured the height of three randomly selected individuals of each species present in each plot unless there were less than three individuals, in which case we measured all individuals. Individuals were not marked, so different individuals may have been measured at different census intervals. To calculate average height of vegetation in each plot we used percent cover data collected in June and August to create an abundance-weighted plot vegetation height. Plot vegetation height was calculated as the sum of the abundance weighted height of each species in the plot, where abundance was quantified as percent cover and height was measured in centimeters. For all but *Lupinus perennis*, percent cover did not differ between the two percent cover census dates and so we used average cover. For *Lupinus perennis*, we used percent cover from June for all census dates in June and July then used August percent cover data for August, September and October census dates.

2.6. Flowering Phenology

We monitored flowering phenology of all focal species at each NDVI census. We used USA-NPN protocols for monitoring (www.usanpn.org/natures_notebook). Here we focus on flowering phenophases due to their potential to influence spectra. Briefly, each species in each plot was scored for whether they had flowers and whether any flowers were open. For each of these phenophases we also scored abundance. For flowers, we scored the number of flowers in the following categories: <3, 3–10, 11–100, >101). For open flowers, we scored the percentage of flowers that were open in the following categories: Less than 5%; 5%–24%; 25%–49%; 50%–74%; 75%–94%; 95% or more.

For data analysis, we took the mid-point of each category, except >101 for which we arbitrarily set as 110. For each species, plot and census we multiplied the number of flowers by the decimal percent of those flowers that were open to get an abundance-weighted number of open flowers per species. These were then summed for each plot giving a total number of open flowers per plot.

2.7. Environmental Conditions

Meteorological conditions (temperature, rainfall) and soil moisture were tracked during the experimental period. Temperature and precipitation records were collected from Cedar Creek weather station (approximately 0.76 km away from the BioDIV experimental plots), while time domain reflectometry (TDR) was used to measure soil moisture at four different depths in a subset of 38 BioDIV experimental plots across all diversity treatment levels. These were not necessarily the same plots as those used for subsampling NDVI but are a representative subset of the ambient conditions in the BioDIV experiment and site. We used the moisture sensor (Trime FM, IMKO GmbH, Ettlingen, Germany), with a 17 cm long probe inserted vertically into the soil inside a 2 m long PVC tube at 4 depths: 3–20 cm, 20–37 cm, 80–97 cm, and 140–157 cm. The sensor was calibrated at two endpoints using the same setup with dry and wet glass beads in a large volume (19 L) following manufacturers instructions.

2.8. Statistical Analysis

Species richness–biomass, species richness–vegetation percent cover and phenology species richness–NDVI relationships were fitted using linear regression model within R software [25]. A multiple linear regression model within R software [25] was applied to fit the NDVI with species richness and vegetation percent cover measurements. We analyzed height data using a two-way ANOVA with species and census as main effects. We used Tukey's HSD to test pairwise contrasts. Phenological data were not normally distributed and transformation did not result in normally distributed data. We therefore used a non-parametric Kruskall-Wallis test to examine the effect of date on the total number of open flowers and then used the Steel-Dwass (non-parametric equivalent to Tukey's HSD) to test pairwise contrasts. These analyses were conducted in JMP® Pro 11.0 (SAS Institute Inc., Cary, NC, USA, 27513).

3. Results

Consistent with previous studies at this site [2], high species richness plots tended to have higher biomass and percent cover, but biomass was more strongly related to species richness than percent cover (Figure 3). Both biomass and vegetation percent cover showed logarithmic relationships with species richness (Figure 3), similar to previous patterns observed at BioDIV [2]. Although the mean vegetation percent cover increased with increasing species richness, the variation of percent cover among low species richness plots was higher than the variation of biomass, with some of the low richness plots having a very high vegetation percent cover, causing a weak (but significant) relationship between species richness and cover (Figure 3b). Species composition clearly affected the species richness—percent cover relationship, as evidenced by the high scatter in percent cover for the monoculture plots. For example, one monoculture plot (*Amorpha canescens*, plot 20 in Table S1 in Supplementary Materials), had the highest vegetation percent cover (95%), but the biomass of this plot was 200 g/m^2, which was only 51.3% of the most productive polyculture, whose richness was 16 (plot 169 in Table S1 in Supplementary Materials). On the other hand, the *Liatris aspera* monoculture plot (plot 129 in Table S1 in Supplementary Materials) has a biomass of 159.97 g/m^2 (41% of the most productive polyculture) while the vegetation percent cover of this plot was only 15%.

NDVI showed a linear relationship with biomass (Figure 4a) but a log relationship with vegetation percent cover (Figure 4b). The NDVI-percent cover relationships had stronger correlations than the NDVI-species richness relationship on both sampling dates (Table 1), illustrating the strong dependence of NDVI on canopy structure. Adding species richness as a variable improved the performance of

the NDVI-percent cover relationships on both sampling dates (Table 1), demonstrating that the NDVI was affected by species composition in addition to canopy structure. These results suggest a potentially confounding effect of vegetation structure (e.g., percent cover) on the NDVI-species richness relationships reported above. NDVI was particularly sensitive to vegetation percent cover in sparse canopies (below 60% cover) and showed less sensitivity to vegetation percent cover in dense canopies (above 60% cover) (Figure 4b), as has been shown by the tendency of NDVI to "saturate" with increasing quantities of vegetation (whether biomass, percent cover or LAI) in previous studies [19]. The NDVI–cover relationship also varied with season, with NDVI values declining between mid-June and early August (Figure 4b). The NDVI and percent cover values were higher earlier in the growing season (19 June) than later (1 August) (Figures 3 and 4), when senescence reduced NDVI (Figure 5).

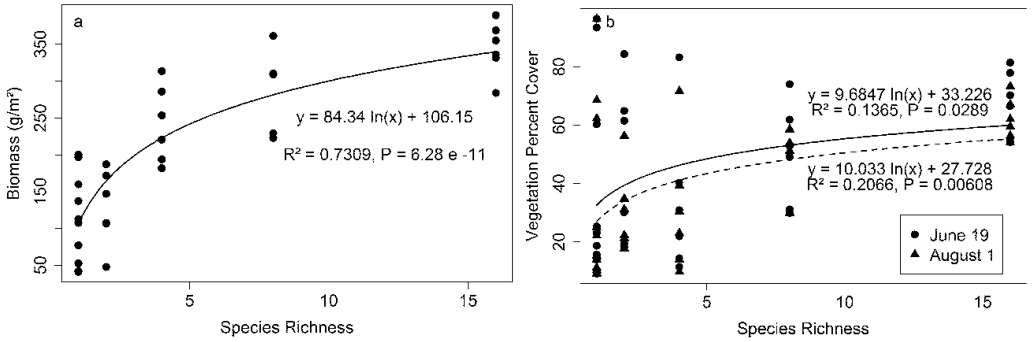

Figure 3. Species richness *versus* biomass (**a**) and vegetation percent cover (**b**). Biomass was measured on 4 August and percent cover was measured on 19 June and 1 August 2014.

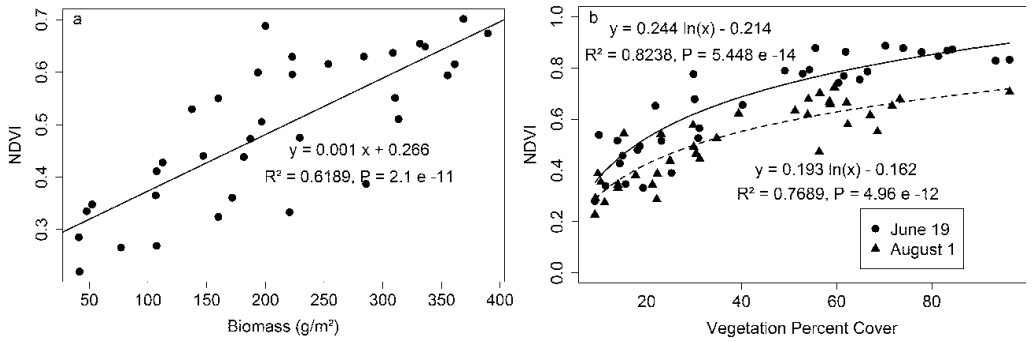

Figure 4. NDVI *versus* biomass (**a**) and vegetation percent cover (**b**). Biomass was measured on 4 August and percent cover was measured on 19 June and 1 August 2014.

Table 1. Dependence of NDVI on species richness and vegetation percent cover. Values shown are multiple linear regression parameters, including intercept, coefficients for log(species richness) and log(percent cover), R^2 and F values. Regressions have degree of freedom = 32. Significant codes: NS, $0.05 < p$, *, $0.05 < p < 0.01$, **, $0.001 < p < 0.01$ and ***, $p < 0.001$. 0619 and 0801 represent the sampling dates (19 June and 1 August 2014).

Date & Model Inputs	Regression Parameters			Overall R^2	Overall F Value
	Intercept	log (Species Richness)	log (Percent Cover)		
0619-Percent cover	−0.21415 **	0	0.24357 ***	0.8238 ***	154.3 ***
0619-Richness	0.53337 ***	0.10391 ***	0	0.3129	15.03 ***
0619-Both	−0.17454 *	0.03296 *	0.22154 ***	0.8486 ***	89.67 ***
0801-Percent cover	−0.14260 *	0	0.18095 ***	0.7387 ***	93.28 ***
0801-Richness	0.37723 ***	0.09317 ***	0	0.4766 ***	30.05 ***
0801-Both	−0.08934NS	0.04280 **	0.15750 ***	0.835 ***	80.98 ***

Reflectance measurements revealed clear NDVI dynamics and subtle changes in the NDVI–diversity relationship that were affected by trends in weather conditions and flowering over the growing season (Figure 5). NDVI showed early-season increases in May and June (Figure 5d), a period of canopy growth and development, as indicated by increases in plant height (Figure 5b). Plants in 16-species plots were significantly taller than those in 8-species plots and both were significantly taller than 4, 2 and 1 species plots (Tukey's HSD, $p < 0.05$). The latter three did not differ from each other (Tukey's HSD, $p > 0.05$).

By August 1, NDVI showed a deep decline accompanied by a coincident decline in surface soil moisture following a period of high temperatures and lack of precipitation, but then recovered briefly during a subsequent period of lower temperature and high precipitation in mid to late August (Figure 5). After this second, smaller August rise, NDVI continued to decline gradually as plants senesced into the fall.

NDVI also appeared to be affected by flowering, with the mid-season NDVI dip coincident with the period of anthesis (flower opening) for many of the dominant species (Figure 5c). The total number of open flowers varied significantly with date ($\chi^2_8 = 65.7$, $p < 0.001$). Pairwise comparisons (Steel-Dwass method) revealed that there were significantly more flowers at the 6 August 2014 census (close to the NDVI dip) than five of the eight other census times. All but 29 May, 21 July and 4 September had significantly lower numbers of flowers.

Over most of the season, NDVI was higher for high-species-richness plots, and the NDVI–species richness relationship shifted over the growing season (Figure 5d). This difference in NDVI for plots with different species richness largely disappeared by October, when plants had largely senesced, at a time of advanced canopy growth (Figure 5b).

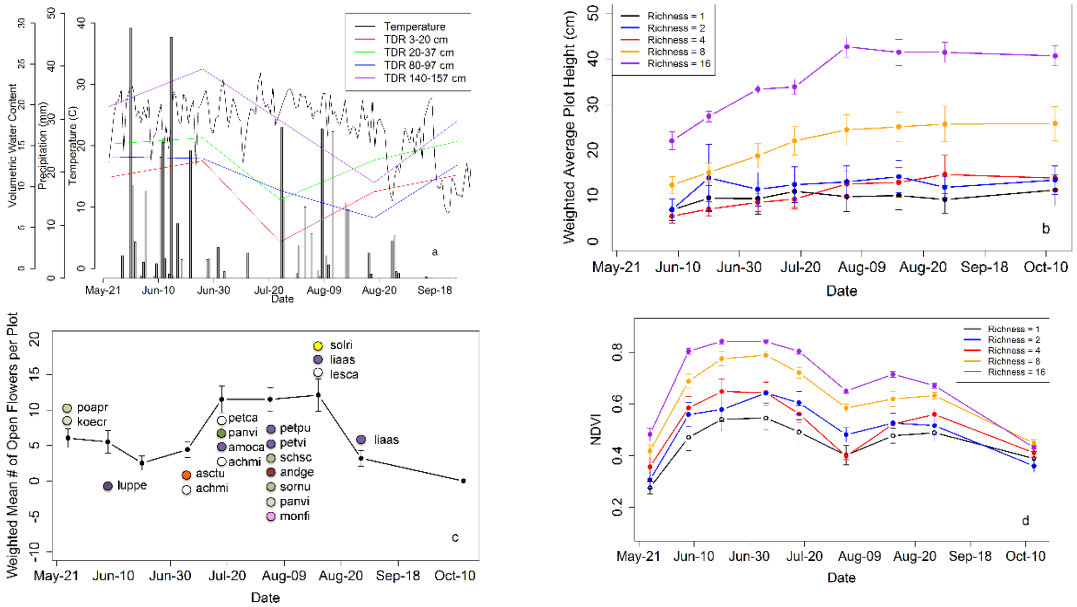

Figure 5. Time series of air temperature (maximum temperature of the day), precipitation, soil moisture expressed as volumetric water content (**a**); weighted average plot height (**b**); weighted mean number of open flowers per plot (**c**) and NDVI plotted by species richness (**d**) over the growing season in 2014. In Figure 5c, the approximate flower color is indicated by the colored circles, and the species names are indicated by 5-letter abbreviations (see Table S2 in Supplementary Materials for full species names).

The seasonal change in the NDVI–species richness relationship is shown in more detail in Figure 6, further demonstrating that plots with high richness tended to have a higher mean NDVI and lower variation in NDVI than plots with low species richness (Figures 6 and 7). The variation of NDVI among the high richness plots became visibly smaller as the growing season progressed (Figure 6).

NDVI showed the strongest relationship with species richness at peak season (Figures 6 and 8 and Table 2). Similarly, whole-plot measurements (Figure 7) based on full-plot sampling (49 measurements) in the middle of the summer showed a clearer trend than any of the individual monthly measurements (Figure 6, Table 2) that were based on smaller sample sizes (17 *vs.* 49 measurements).

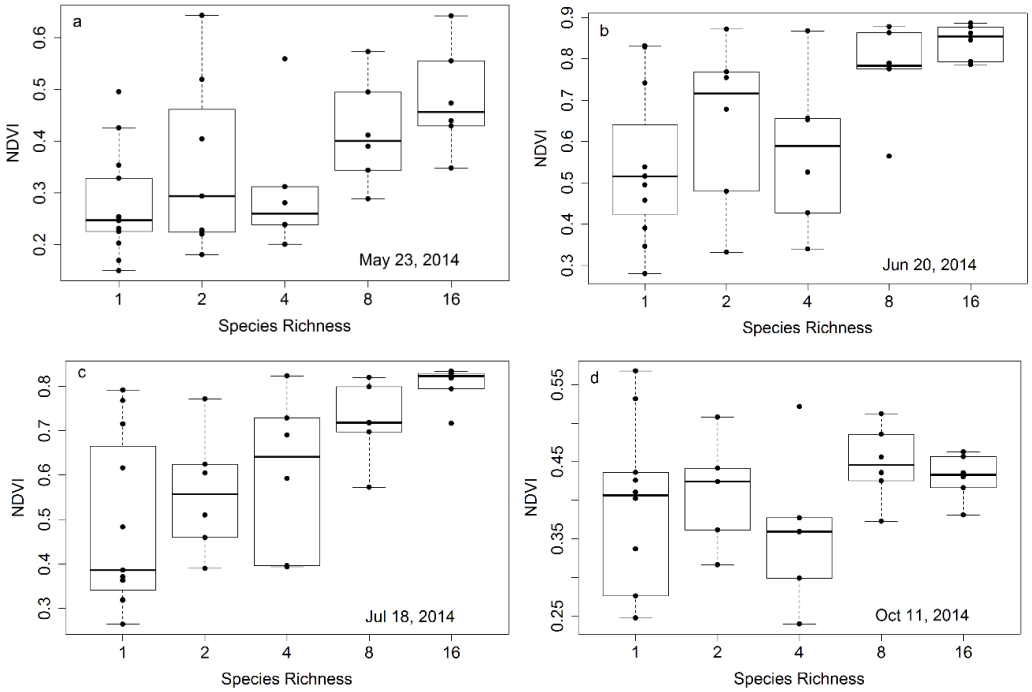

Figure 6. Representative examples of NDVI *versus* species richness at four time points (plots **a**–**d**) in the 2014 growing season. These figures were derived from plot subsamples (17 measurements along the north most row of each plot) for 35 plots. Species richness represents the planted number of species per plot. Each richness treatment had a sample size of 6, except monoculture plots, which had a sample size of 11. In this figure, box plots were overlaid on actual data points (dots) that represent the average values for each plot. The regression statistics are provided in Table 1.

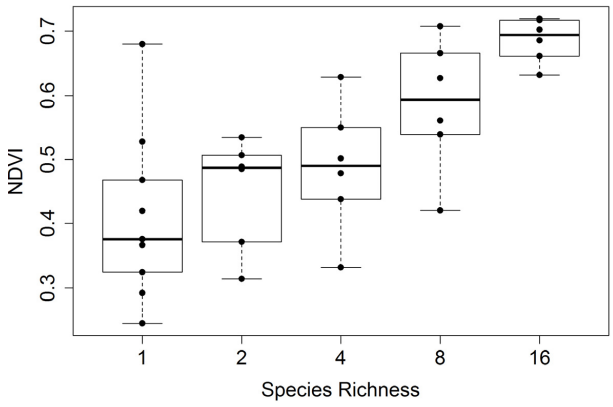

Figure 7. Mid-season whole-plot NDVI *versus* species richness (collected over several dates spanning 23 July to 3 August 2014). For this figure, 49 (7 m × 7 m) of the 81 measurements in the center of each plot were used to calculate the average reflectance and NDVI, yielding a more representative sampling than shown in Figure 6. Species richness represents the planted number of species per plot. Each richness treatment had a sample size of 6, except monoculture plots, which had a sample size of 9. In this figure, box plots were overlaid on actual data points (dots) that represent the average values for each plot. The regression statistics are provided in Table 2.

Table 2. Species richness–NDVI relationships for various dates in 2014 compared to the whole plot results obtained at mid-summer (23 July–2 August 2014).

Sampling	Regression Equation	R^2	p Value
23 May	y = 0.0132x + 0.2821	0.2587	0.001
8 June	y = 0.0211x + 0.4841	0.3312	0.0003
20 June	y = 0.0199x + 0.548	0.3137	0.0005
06 July	y = 0.0193x + 0.5651	0.3325	0.0003
18 July	y = 0.0207x + 0.5022	0.374	9.51×10^{-5}
4 August	y = 0.0178x + 0.3909	0.4728	5.04×10^{-6}
21 August	y = 0.0157x + 0.4725	0.3789	0.0001
5 September	y = 0.0119x + 0.4957	0.2737	0.001
11 October	y = 0.0034x + 0.3854	0.05	0.209
Whole-plot Sampling	y = 0.0177x + 0.4114	0.5136	6.07×10^{-7}

A more complete summary of the effects of sample date and size on the NDVI-species richness relationship is provided in Table 2, clearly illustrating that the strongest relationships were obtained towards mid-summer when plants were fully mature and before the onset of senescence, and that larger sample sizes based on whole-plot data improved the relationships. The seasonal pattern in the NDVI-species richness relationship (expressed as R^2 values) can be compared to the NDVI time trend, showing a peak in the correlation during the mid-season dip in NDVI, a time of warm, dry conditions and peak anthesis (Figures 5 and 8).

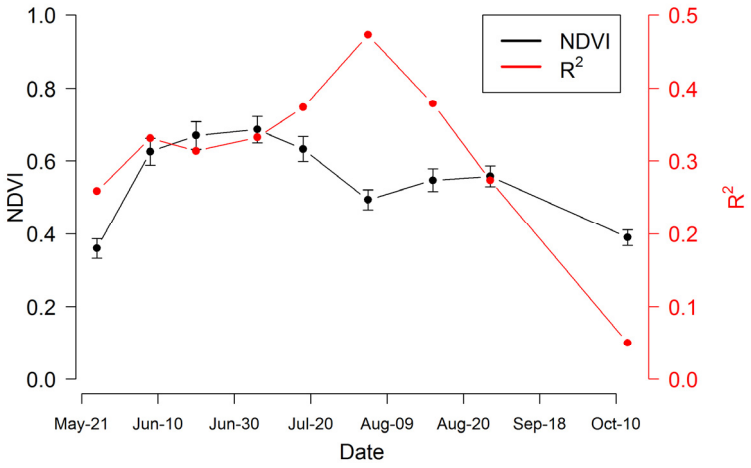

Figure 8. Time series of NDVI (black line) and R^2 of the NDVI-species richness regression (red line) over the growing season in 2014. NDVI was the average value (±SEM) of all the plots on each sampling date.

4. Discussion

4.1. Biomass–NDVI Relationship

In this study, the significant relationship between biomass and NDVI (Figure 4) agrees with previous research, and has been discussed in multiple systems from both theoretical [26] and empirical approaches [19]. NDVI provides a rapid and non-destructive method of estimating biomass and percent cover, providing an empirical relationship between spectral information and biomass and percent cover [27]. Both vegetation percent cover and biomass have been broadly used as surrogates of vegetation productivity [10], especially in grasslands [28]. Using NDVI, remote sensing can assess continuous dynamics of biomass productivity over the growing season at a large scale.

The correlation between NDVI and biomass in our study, while significant, was lower than is often reported [19]. One reason for this scatter is that we did not harvest the biomass from the

same plot location as NDVI sampling, but assumed that the plots were homogeneous in order to get continuous phenology NDVI measurements in the whole growing season. The NDVI–biomass relationship (Figure 4) could have been improved by matching the exact locations of NDVI and biomass sampling [19] but this would have precluded time-series analysis of NDVI phenology. Variation in the NDVI–biomass relationship can also be caused by variation in canopy structure, with different canopy architectures having slightly different NDVI–biomass relationships. Another reason for the scatter may be that NDVI is more closely related to $fPAR_{green}$, a measure of light absorption by green canopy material and hence potential production [19,29], than biomass *per se*. Like biomass harvesting, $fPAR_{green}$ measurement is also destructive and was not measured in our study (but can be inferred from NDVI).

4.2. Productivity–Richness Relationship

The productivity-biodiversity relationship is a much-discussed topic in the ecological literature [2,6–8,30], and undoubtedly is influenced by many factors. Biodiversity can affect the production of ecosystems due to the complementary roles played by different species [3]. For example, adding species within a community can enhance the ability of vegetation to capture resources [31]. Similar to what has been previously reported with the biomass-species richness relationships [2], the NDVI-species richness relationship tended to approach saturation at the high richness end (8 to 16 species). This may be because when all functional groups are present, the addition of species with redundant function has little effect on ecosystem properties [9].

Selection effects result from the increased probability of adding a productive species in higher diversity polycultures and can also contribute to the explanation of high biomass in polycultures. In the Cedar Creek BioDIV experiment, both selection effects and complementarity of species have been shown to affect the community productivity [23,32]. Our goal in this study was not to further analyze the respective contributions of selection and complementarity effects [4], but rather to use a remotely sensed measure of vegetation to examine the dynamics of the biodiversity–productivity relationship through time. We note that most of the productive monocultures may have equivalent or even higher biomass than some of the polycultures (shown as higher NDVI in some of the monoculture in our study), that species express different growth and phenological stages at any given point in time (Figure 5), and that the most productive species can change though time within one growing season (data not shown). Moreover, it is unlikely that a monoculture can be more productive than a diverse community when considering a long time span [31]. When a long time period (>10 years) is considered, accumulation of complementarity effects can dominate the productivity–richness relationship and lead to a more positive relationship [23,32].

At present, remote sensing does not necessarily inform the mechanisms underlying the biodiversity-productivity relationship. However, the non-destructive nature of remote assessment assists our understanding of the dynamics of the richness–productivity relationship through time and in relationship to environmental constraints by permitting repeated landscape-level assessments beyond the scope of typical field plots. In our study, only a small number of species was considered at a local scale, but these methods can also be readily applied to larger regions. In a parallel study of prairie grassland in southern Alberta, Wang *et al.* [33] found a similar, positive relationship between productivity and biodiversity over a large landscape using airborne imaging spectrometry coupled with field sampling. Understanding the mechanisms underlying the richness–productivity relationship, while beyond the scope of this particular study, can help maintain and conserve biodiversity [10].

4.3. Richness-Percent Cover and Effects

In this study, NDVI was affected by both species richness and vegetation percent cover, and vegetation percent cover had a stronger effect than species richness (Table 1). The Cedar Creek BioDIV prairie ecosystem experiment is maintained at nominal species richness via burning and weeding every year. Fecundity and dispersal feedbacks over time have resulted in patchiness and low percent cover

of some of the low richness plots [34]. As a result, the low richness plots may have increased exposed soil and moss-covered patches. This factor, in addition to vegetation composition effects on NDVI, may have contributed to the reduced NDVI in low richness plots. Further studies could focus on plots with different species richness but similar vegetation percent cover, or on manipulating different species composition at same richness level to control for plant density, to better understand how species richness, cover and composition affect the optical diversity signal separately. The potential to apply remote sensing to address these questions over larger regions and natural landscapes is high [33] and critical to understanding these relationships in natural systems, and ultimately to managing ecosystems for resiliency in the face of rapid global change.

4.4. Seasonal NDVI Variation

Many factors, including changing canopy display, leaf pigmentation, and flowering, can all influence NDVI. In our study, the drop of NDVI in early August was coincident with the high temperature and lack of precipitation in late July (Figure 5). In the short term, water stress can affect NDVI by causing vegetation wilting and leaf rolling. These changes in canopy structure tend to decrease vegetation visibility and increase soil visibility to the sensor, decreasing NIR reflectance and increasing visible reflectance, and thus reducing NDVI. This temporary effect of water stress can be reversed by precipitation, allowing vegetation to recover to some extent, and this helps explain the early August NDVI dip and subsequent increase (Figure 5). Similarly, the mid-season NDVI drop was coincident with anthesis, the time of maximum flower opening, which has also been shown to reduce NDVI depending upon flower color and its influence on the reflectance spectrum [34–36].

4.5. Sample Size

Sample size also affects the NDVI-richness relationship. In our study, the mid-season whole plot results that had a higher sample size (n = 49) showed a stronger NDVI-richness relationship than any of the repeated monthly measurements in a similar subset of plots with a smaller sample size (n = 17) (Figures 6 and 7 Table 2). Most likely, the whole-plot measurements were more representative of the Cedar Creek BioDIV study than the time-series results that only included a subsample of the full plot areas. Similarly, previous studies [37] and models [38] showed increasing accuracy with increasing number of sampling strategies. Considering that remote sensing can readily obtain large regions while providing a systematic view of the Earth at regular time intervals, it holds the promise of becoming a feasible, convenient and cost-effective way to conduct biodiversity research [39].

4.6. Seasonality of the NDVI-Species Richness Relationship

Compared to the spatial patterns of biodiversity, less attention has been paid to the seasonal patterns of biodiversity [40] or the effect of phenology on the ability to assess biodiversity with remote sensing. In our study, the NDVI-richness relationship was dynamic and the best regression between NDVI and species richness occurred near peak season, although the exact reasons for this deserve further study. This dynamic relationship was most likely affected by canopy development, as well as by prevailing conditions (mid-season warm, dry conditions) and flowering phenology (timing of anthesis). While both short-term drought and mid-season anthesis clearly reduced NDVI, their effect on the NDVIbiodiversity patterns was less clear, and could have even enhanced this relationship, as illustrated by the enhanced NDVI-biodiversity correlations at mid-season (Figures 6–8 Table 2), or at least not interfered with it. Multi-year data may be helpful to separate the confounding effects of short term drought and anthesis on NDVI–biodiversity relationship because the seasonal meteorology can vary year to year. The exact impact of these multiple factors on the timing of the NDVI–biodiversity relationship, while beyond the scope of this study, might yield additional insights into the mechanisms driving the productivity–biodiversity relationship.

5. Conclusions

Remote sensing provides an efficient and inexpensive way to assess biomass and biodiversity. This study further confirms earlier studies at this site, and illustrates the potential of remote sensing to assess the diversity–productivity relationship. The Cedar Creek experiments provide a convenient test of this relationship in a human-maintained prairie ecosystem. Considering the two hypotheses proposed in the introduction, this study shows that NDVI can be related to species richness, but it is also strongly affected by other factors, including canopy structure (cover or biomass) and short-term water stress and shifting flowering patterns that can confound the NDVI-richness relationship. Interestingly, the strongest NDVI–biodiversity relationship occurred in mid-summer, when NDVI showed a temporary decline associated with warm, dry conditions and anthesis.

While remote sensing has the potential to be used in biodiversity assessment, it also adds additional capabilities and complexity by being able to assess this diversity at multiple scales. Further work should address the optical-biodiversity relationship in more detail, in part by addressing the scale-dependence. As well, future studies should take advantage of the full spectral power of imaging spectrometry to evaluate the diversity–productivity relationship for a larger variety of ecosystems.

Supplementary Materials: The following are available online at www.mdpi.com/2072-4292/8/2/128, Table S1: Species richness and composition of each plot used in this study. The species abbreviations and identities are summarized in Table S2. Table S2: Species abbreviations and identities in Table S1.

Acknowledgments: We thank staff at the Cedar Creek Ecosystem Science Reserve, particularly Troy Mielke and Kally Worm, and research assistant, Jonathan Anderson. We also thank Aidan Mazur and Melanie Sitten from University of Wisconsin-Madison for helping collect the whole plot reflectance data. This study was supported by a NASA and NSF grant DEB-1342872 to J. Cavender-Bares, a NSF-LTER grant to D. Tilman, J. Cavender-Bares and R. Montgomery DEB-1234162 and by iCORE/AITF and NSERC grants to J. Gamon, and a China Scholarship Council fellowship to R. Wang.

Author Contributions: R.W. was the primary author, and J.G., J.C.-B., R.A.M., P.T., and A.Z. all contributed to the writing; R.W., J.G., K.B. collected the optical data; R.A.M. contributed flowering and height (phenology) data; R.W. provided most of the data analysis, with a contribution from R.A.M. on the analysis of phenology data; R.W., J.G., J.C.-B., R.A.M., D.T. contributed to the design of the experiment.

Conflicts of Interest: The authors declare no conflict of interest.

References

1. Tilman, D.; Reich, P.B.; Knops, J.; Wedin, D.; Mielke, T.; Lehman, C. Diversity and productivity in a long-term grassland experiment. *Science* **2001**, *294*, 843–845. [CrossRef] [PubMed]
2. Tilman, D. The Influence of functional diversity and composition on ecosystem processes. *Science* **1997**, *277*, 1300–1302. [CrossRef]
3. Tilman, D.; Wedin, D.; Knops, J. Productivity and sustainability influenced by biodiversity in grassland ecosystems. *Nature* **1996**, *379*, 718–720. [CrossRef]
4. Loreau, M.; Hector, A. Partitioning selection and complementarity in biodiversity experiments. *Nature* **2001**, *412*, 72–76. [CrossRef] [PubMed]
5. Lehman, C.L.; Tilman, D. Biodiversity, stability, and productivity in competitive communities. *Am. Nat.* **2000**, *156*, 534–552. [CrossRef]
6. Huston, M.A. Hidden treatments in ecological experiments: Re-evalutating the ecosystem function of biodiverstiy. *Oecologia* **1997**, *110*, 449–460. [CrossRef]
7. Adler, P.B.; Seabloom, E.W.; Borer, E.T.; Hillebrand, H.; Hautier, Y.; Hector, A.; Harpole, W.S.; Halloran, L.R.O.; Grace, J.B.; Anderson, T.M.; *et al*. Productivity is a poor predictor of plant species richness. *Science* **2011**, *1750*, 1750–1754. [CrossRef] [PubMed]
8. Fraser, L.H.; Pither, J.; Jentsch, A.; Sternberg, M.; Zobel, M.; Askarizadeh, D.; Bartha, S.; Beierkuhnlein, C.; Bennett, J.A. Worldwide evidence of a unimodal relationship between productivity and plant species richness. *Science* **2015**, *349*, 302–306. [CrossRef] [PubMed]
9. Waide, R.B.; Willig, M.R.; Steiner, C.F.; Mittelbach, G.; Gough, L.; Dodson, S.I.; Juday, G.P.; Parmenter, R. The relationship between productivity and species richness. *Annu. Rev. Ecol. Syst.* **1999**, *30*, 257–300. [CrossRef]

10. Mittelbach, G.G.; Steiner, C.F.; Scheiner, S.M.; Gross, K.L.; Reynolds, H.L.; Waide, R.B.; Willig, M.R.; Dodson, S.I.; Gough, L. What is the observed relationship between species richness and productivity? *Ecology* **2001**, *82*, 2381–2396. [CrossRef]
11. Reich, P.B.; Hobbie, S.E. Decade-long soil nitrogen constraint on the CO_2 fertilization of plant biomass. *Nat. Clim. Chang.* **2013**, *3*, 278–282. [CrossRef]
12. Isbell, F.; Craven, D.; Connolly, J.; Loreau, M.; Schmid, B.; Beierkuhnlein, C.; Bezemer, T.M.; Bonin, C.; Bruelheide, H.; de Luca, E.; *et al*. Biodiversity increases the resistance of ecosystem productivity to climate extremes. *Nature* **2015**, *526*, 574–577. [CrossRef] [PubMed]
13. Tilman, D.; El Haddi, A. Drought and biodiversity in Grasslands. *Oecologia* **1992**, *89*, 257–264. [CrossRef]
14. Bork, E.W.; West, N.E.; Price, K.P.; Walker, J.W. Rangeland cover component quantification using broad (TM) and narrow-band (1.4 NM) spectrometry. *J. Range Manag.* **1999**, *52*, 249–257. [CrossRef]
15. Booth, D.T.; Tueller, P.T. Rangeland monitoring using remote sensing. *Arid Land Res. Manag.* **2003**, *17*, 455–467. [CrossRef]
16. Piñeiro, G.; Oesterheld, M.; Paruelo, J.M. Seasonal variation in aboveground production and radiation-use efficiency of temperate rangelands estimated through remote sensing. *Ecosystems* **2006**, *9*, 357–373. [CrossRef]
17. Clark, D.A.; Brown, S.; Kicklighter, D.W.; Chambers, J.Q.; Thomlinson, J.R.; Ni, J. Measuring net primary production in forest: Concepts and field methods. *Ecol. Appl.* **2001**, *11*, 356–370. [CrossRef]
18. Gamon, J.A.; Field, C.B.; Roberts, D.A.; Ustin, S.L.; Valentini, R. Functional patterns in an annual grassland during an AVIRIS overflight. *Remote Sens. Environ.* **1993**, *44*, 239–253. [CrossRef]
19. Gamon, J.A.; Field, C.B.; Goulden, M.L.; Griffin, K.L.; Hartley, A.E.; Joel, G.; Penuelas, J.; Valentini, R. Relationships between NDVI, canopy structure, and photosynthesis in three californian vegetation types. *Ecol. Appl.* **1995**, *5*, 28–41. [CrossRef]
20. Tucker, C.J. Red and photographic infrared linear combinations for monitoring vegetation. *Remote Sens. Environ.* **1979**, *8*, 127–150. [CrossRef]
21. Tilman, D.; Reich, P.B.; Knops, J.M.H. Biodiversity and ecosystem stability in a decade-long grassland experiment. *Nature* **2006**, *441*, 629–632. [CrossRef] [PubMed]
22. Mittelbach, G.G. Biodiversity and ecosystem functioning. In *Community Ecology*; Mittelbach, G.G., Ed.; Sinauer Associates, Inc.: Sunderland, MA, USA, 2012; Chapter 3; pp. 41–62.
23. Reich, P.B.; Tilman, D.; Isbell, F.; Mueller, K.; Hobbie, S.E.; Flynn, D.F.B.; Eisenhauer, N. Impacts of biodiversity loss escalate through time as redundancy fades. *Science* **2012**, *336*, 589–592. [CrossRef] [PubMed]
24. Gamon, J.A.; Cheng, Y.; Claudio, H.; MacKinney, L.; Sims, D.A. A mobile tram system for systematic sampling of ecosystem optical properties. *Remote Sens. Environ.* **2006**, *103*, 246–254. [CrossRef]
25. R Core Team. *R: A Language and Environment for Statistical Computing*; R Foundation for Statistical Computing: Vienna, Austria, 2015.
26. Sellers, P.J. Canopy reflectance, photosynthesis, and transpiration. II—The role of biophysics in the linearity of their interdependence. *Remote Sens. Environ.* **1987**, *21*, 143–183. [CrossRef]
27. Gitelson, A.A.; Kaufman, Y.J.; Stark, R.; Rundquist, D. Novel algorithms for remote estimation of vegetation fraction. *Remote Sens. Environ.* **2002**, *80*, 76–87. [CrossRef]
28. Scurlock, J.M.O.; Johnson, K.; Olson, R.J. Estimating net primary productivity from grassland biomass dynamics measurements. *Glob. Chang. Biol.* **2002**, *8*, 736–753. [CrossRef]
29. Gitelson, A.A.; Gamon, J.A. The need for a common basis for defining light-use efficiency: Implications for productivity estimation. *Remote Sens. Environ.* **2015**, *156*, 196–201. [CrossRef]
30. Wardle, D.A. Is "sampling effect" a problem for experiments investigating biodiversity-ecosystem function relationships? *Oikos* **1999**, *87*, 403–407. [CrossRef]
31. Cardinale, B.J.; Wright, J.P.; Cadotte, M.W.; Carroll, I.T.; Hector, A.; Srivastava, D.S.; Loreau, M.; Weis, J.J. Impacts of plant diversity on biomass production increase through time because of species complementarity. *Proc. Natl. Acad. Sci. USA* **2007**, *104*, 18123–18128. [CrossRef] [PubMed]
32. Fargione, J.; Tilman, D.; Dybzinski, R.; Lambers, J.H.R.; Clark, C.; Harpole, W.S.; Knops, J.M.H.; Reich, P.B.; Loreau, M. From selection to complementarity: Shifts in the causes of biodiversity-productivity relationships in a long-term biodiversity experiment. *Proc. Biol. Sci.* **2007**, *274*, 871–876. [CrossRef] [PubMed]
33. Wang, R.; Gamon, J.A.; Emmerton, C.A.; Li, H.; Nestola, E.; Pastorello, G.Z.; Menzer, O. Integrated analysis of productivity and biodiversity in a southern Alberta prairie. *Remote Sens.* **2016**. under review.

34. Naeem, S.; Knops, J.M.; Tilman, D.; Howe, K.M.; Kennedy, T.; Gale, S. Plant diversity increases resistance to invasion in the absence of covarying extrinsic factors. *Oikos* **2000**, *91*, 97–108. [CrossRef]
35. Joel, G.; Gamon, J.A.; Field, C.B. Production efficiency in sunflower: The role of water and nitrogen stress. *Remote Sens. Environ.* **1997**, *62*, 176–188. [CrossRef]
36. Shen, M.; Chen, J.; Zhu, X.; Tang, Y.; Chen, X. Do flowers affect biomass estimate accuracy from NDVI and EVI? *Int. J. Remote Sens.* **2010**, *31*, 2139–2149. [CrossRef]
37. Magurran, A.E. *Measuring Biological Diversity*; Blackwell Publishing: Malden, MA, USA, 2004.
38. Pavlick, R.; Drewry, D.T.; Bohn, K.; Reu, B.; Kleidon, A. The Jena Diversity-Dynamic Global Vegetation Model (JeDi-DGVM): A diverse approach to representing terrestrial biogeography and biogeochemistry based on plant functional trade-offs. *Biogeosciences* **2013**, *10*, 4137–4177. [CrossRef]
39. Nagendra, H. Using remote sensing to assess biodiversity. *Int. J. Remote Sens.* **2001**, *22*, 2377–2400. [CrossRef]
40. Magurran, A.E. Diversity over time. *Folia Geobot.* **2008**, *43*, 319–327. [CrossRef]